American Journal of Botany

RESEARCH ARTICL

Root vascular traits differ systematically between African savanna tree and grass species, with implications for water use

Isabel K. Wargowsky[1], Julienne E. NeSmith[1], and Ricardo M. Holdo[1,2,3]

Manuscript received 2 July 2020; revision accepted 17 September 2020.

[1] Odum School of Ecology, University of Georgia, Athens, GA 30602, USA

[2] School of Animal Plant and Environmental Sciences, University of the Witwatersrand, Johannesburg 2050, South Africa

[3] Author for correspondence (e-mail: rholdo@uga.edu)

Citation: Wargowsky. I. K., J. E. NeSmith, and R. M. Holdo. 2021. Root vascular traits differ systematically between African savanna tree and grass species, with implications for water use. *American Journal of Botany* 108(1): 1–8.

doi:10.1002/ajb2.1597

PREMISE: Belowground functional traits play a significant role in determining plant water-use strategies and plant performance, but we lack data on root traits across communities, particularly in the tropical savanna biome, where vegetation dynamics are hypothesized to be strongly driven by tree–grass functional differences in water use.

METHODS: We grew seedlings of 21 tree and 18 grass species ($N = 5$ individuals per species) from the southern African savanna biome under greenhouse conditions and collected fine-root segments from plants for histological analysis. We identified and measured xylem vessels in 539 individual root cross sections. We then quantified six root vascular anatomy traits and tested them for phylogenetic signals and tree–grass differences in trait values associated with vessel size, number, and hydraulic conductivity.

RESULTS: Grass roots had larger root xylem vessels than trees, a higher proportion of their root cross-sectional area comprised vessels, and they had higher estimated axial conductivities than trees, while trees had a higher number of vessels per root cross-sectional area than grasses did. We found evidence of associations between trait values and phylogenetic relatedness in most of these traits across tree species, but not grasses.

CONCLUSIONS: Our findings support the hypothesis that grass roots have higher water transport capacity than tree roots in terms of maximum axial conductivity, consistent with the observation that grasses are more "aggressive" water users than trees under conditions of high soil moisture availability. Our study identifies root functional traits that may drive differential responses of trees and grasses to soil moisture availability.

KEY WORDS root conductivity; savanna vegetation dynamics; tree-grass coexistence; water uptake; xylem anatomy.

Savannas represent one of the few global biomes where trees and grasses are co-dominant (Scholes and Walker, 1993; Sankaran et al., 2004). The key mechanisms allowing the coexistence of these two major plant functional types continue to be debated (Sankaran et al., 2004; Staver et al., 2011a; Ratajczak et al., 2017). Models explaining coexistence fall largely into two categories: those assuming that competitive exclusion would eliminate either trees or grasses in the absence of disturbance or other top–down drivers such as herbivory, and those that assume that niche differences—primarily in relation to water use—lead to stable coexistence (Sankaran et al., 2004). Niche-based models assume that trees and grasses differ in terms of important functional traits associated with water acquisition and use, such as water-use efficiency, maximum transpiration, drought tolerance, and/or rooting depth (Eagleson and Segarra, 1985; van Wijk and Rodriguez-Iturbe, 2002; Xu et al., 2015). Despite the focus on niche-based mechanisms, however, there is a surprising lack of comparative data on functional traits in trees vs. grasses for any given savanna ecosystem. Furthermore, there is a particular paucity of data on belowground traits, even though roots play a significant role in driving plant water relations (Fort et al., 2017; Bakker et al., 2019).

Water is a key limiting resource in savannas (Scholes and Walker, 1993; Sankaran et al., 2005), and therefore, root functional traits associated with water acquisition and transport are likely to be of primary importance for understanding the relative response of trees and grasses to fluctuations in water availability. One root functional

trait that has been widely studied in savanna trees and grasses is rooting depth, given the early focus on rooting depth differences between trees and grasses as a driver of coexistence (Walter, 1971; Walker and Noy-Meir, 1982). More recently, studies have shown theoretically that coexistence can be influenced by differences in demographic rates and drought tolerance between trees and grasses (van Wijk and Rodriguez-Iturbe, 2002); a trade-off between growth rate under wet conditions and drought tolerance (Xu et al., 2015); and the differential abilities of trees and grasses to exploit topsoil water via hydraulic lift (Yu and D'Odorico, 2015), among other examples (Scholes and Walker, 1993; Rodríguez-Iturbe et al., 1999). One trait category in particular stands out: the ability to capture soil moisture when it is readily available (Xu et al., 2015). In most savanna models, grasses are assumed to be the more "aggressive" water users, with high transpiration rates and hydraulic conductances (Xu et al., 2015), but there is a lack of data to assess the extent of this variation, particularly in the African savanna biome. Generally, most functional trait data used to parameterize tree–grass models in savannas derive from a limited number of sources (notably, the Scholes and Walker [1993] Nylsvlei synthesis from South Africa), and then from a relatively small number of tree and grass species.

Plant hydraulic conductance integrates many organ-specific elements (Sperry et al., 2016; Venturas et al., 2018), but roots ultimately play the most critical role in terms of water-acquisition capacity by virtue of their location at the plant–soil interface. In a far-ranging study of root traits, Ma et al. (2018) demonstrated extensive differences in a number of root traits (such as specific root length and diameter) between woody and herbaceous species worldwide. Two notable gaps in this study, however, are the lack of data on root xylem traits and the poor representation of savanna tree and grass species (Ma et al., 2018). Root vessel architecture plays a key role in water transport (Lambers et al., 1998; Wang et al., 2015), and xylem anatomy is recognized as an important aspect of species' ecohydrological niches (Lambers et al., 1998; Zanne et al., 2010; Robert et al., 2017). Vessel anatomy remains understudied in savanna species, however. To the best of our knowledge, no systematic comparisons of tree and grass xylem vessel characteristics have been conducted to date. In addition to testing for tree–grass differences in vessel anatomy, it is important to analyze vascular traits in the context of phylogenetic relationships to understand their evolutionary history (e.g., the extent to which they are evolutionarily conserved or not). In addition, if clades are associated with trait values, inferences may be made about trait values for unobserved species based on their place in the phylogeny.

In the present greenhouse study, we compared the root xylem anatomy of ~40 co-occurring tree and grass species from a South African savanna ecosystem. Assuming that savanna grasses have higher transport capacity than trees for a given investment in biomass (Bond, 2008; Xu et al., 2015), we hypothesized that grasses have larger root xylem vessels and a higher theoretical root conductivity than trees, potentially allowing them to more effectively exploit available water during wet conditions.

MATERIALS AND METHODS

Study species and growing conditions

We obtained seeds of 21 tree species and 18 grass species (including two subspecies of *Aristida congesta*) from the southern Africa savanna biome as a source of plant material. We focused on species that are relatively common in the lowveld savanna of Kruger National Park and the nearby Wits Rural Facility field station in Limpopo Province, South Africa. We obtained most ($N = 15$) of our tree seeds from a commercial supplier (Silverhill Seeds, Cape Town, South Africa) in 2017. These seeds are collected from wild trees in the field within species ranges in South Africa. We collected seeds of four additional tree species plus all grass species within Wits Rural Facility in February–April 2018 (Appendix S1). We also obtained seeds of a dominant Miombo woodland tree (*Brachystegia spiciformis*), collected in Zimbabwe.

We grew tree and grass seedlings (target: $N = 5$ per species) in the Botany Greenhouse at the University of Georgia between January and October 2018 (Appendix S1). Before planting, we used a razor blade to scarify tree seeds with hard coats and then soaked all tree seeds in tap water for 48 h. We staggered the planting dates of trees (median date: 30 January) and grasses (median date: 21 June) to accommodate for broad differences in growth rate between the two functional groups. In a previous pilot experiment, we had determined that it took tree seedlings ~3–6 months to reach our target height (about the depth of the container, 37 cm), while grasses took ~1–2 months to reach a similar height following transplantation. We planted all seeds in seedling trays filled with soilless media (Fafard 3B, Sun Gro Horticulture, Agawam, MA, USA), and watered them daily to saturation. Following germination, we transplanted seedlings into 20-L containers after they had produced at least one fully expanded true leaf (tree and grass median transplant date: 21 February and 28 June, respectively). We placed the containers in randomly selected locations on greenhouse benches. We filled the containers with rinsed river sand over a slim layer of #47 gravel and watered them daily. Post-transplant, we applied 14 g of slow release fertilizer (Osmocote 14-14-14) and 4 g each of gypsum and limestone to each pot. The staggered planting and transplanting allowed us to harvest plant material for both functional groups concurrently (tree and grass median harvest dates: 16 August and 27 August, respectively). We quantified temperature and relative humidity in the greenhouse using a VP-4 humidity and temperature sensor connected to an Em50 datalogger (Meter Group, Pullman, WA, USA). We quantified solar radiation (in the spectral range 380–1120 nm) inside the greenhouse roof with a PYR pyranometer (Meter Group) connected to the Em50. Datalogger failure led to data loss during the peak growing season (June–August). Conditions in the following year during this same period were as follows: the mean daily minimum and maximum temperatures were 22.1 and 33.7°C, respectively, relative humidity ranged between 32 and 98% (with a mean of 74%), and mean daily solar radiation between 08:00 and 20:00 hours was 540 W m^{-2} (~2470 μmol m^{-2} s^{-1}).

Root harvest and characterization of vessel anatomy

We harvested trees and grasses once their height became comparable to the container height, except in the case of the slowest-growing tree species, which we harvested no later than October 2018. Our goal was to harvest tree and grass seedlings of comparable size (e.g., biomass or leaf area) because models of tree–grass dynamics tend to focus on biomass or size differences between trees and grasses rather than on age structure (Eagleson and Segarra, 1985; Staver et al., 2011b; Xu et al., 2015). Moreover, it is extremely difficult to age savanna trees and grasses in the field; in particular, what often appear to be tree seedlings are in fact suppressed "gullivers" that can be

years or decades old (Boaler and Sciwale, 1966; Higgins et al., 2000). Still, trait values are bound to vary with plant age, which posed a potential challenge in our case because of the different growth rates of trees and grasses. Many of our tree seedlings would have been very small if we had harvested them at an age where grasses reach the target height. Conversely, our grasses might have become pot-bound if we had delayed their harvest to coincide with the age of our tree harvest. Our grasses were therefore younger than our tree seedlings (on average) at harvest, and in the data analysis stage, we assessed whether this age difference was likely to bias our findings.

We used plant height as a rule of thumb for assessing readiness for harvest, but then measured total plant leaf area as a postharvest check on size differences. Upon harvest, we separated all leaves and immediately scanned a sample of fresh leaves on a flatbed scanner for leaf area determination using ImageJ (Schneider et al., 2012). We separately dried (at 65°C for 48 h) and weighed both the leaf sample and the leaf remainder for each plant and used the specific leaf area value calculated from the sample to estimate total plant leaf area. During the harvest, we also rinsed all roots to remove soil, then immediately clipped multiple segments (<5 cm in length) of fine roots (<2 mm in diameter) per plant. We did not categorize roots by order, but rather focused on collecting segments of similar diameter for both trees and grasses. For each individual plant, we placed root segments into 15-mL vials filled with formaldehyde–alcohol–acetic acid (FAA) fixative solution (10% formaldehyde [37%], 50% ethanol [95%], 5% glacial acetic acid, and 35% deionized water, all v/v; Wang et al., 2015). Shortly following harvest (up to 2 d), we placed uncapped vials into a desiccator attached to a vacuum pump to remove air bubbles and facilitate penetration of the fixative into root vessels. Uncapped vials remained in the desiccator for 24 h before they were capped and cold-stored (4°C) until preparation for histology. In late 2018, we transferred root subsets from the FAA vials to vials filled with 70% ethanol, 24 h before histological work. The transfer to ethanol dehydrates the sample before embedding and sectioning (Wang et al., 2015). We retrieved up to four root segments from each prepared vial, cut cross sections approximately 2 mm long, and set the sections into embedding cassettes. Any roots that were too small to remain properly oriented we lodged into potato slices. The transverse sections within each cassette were then embedded into a single paraffin block and sliced (4–12 μm thick) using a microtome at the Histology Laboratory in the Department of Pathology in the College of Veterinary Medicine at the University of Georgia. Each slice was mounted on a microscope slide and stained with safranin O (4 g) and fast green (0.23 g) solution. Safranin O is a basic dye that will stain red any acidic features of the tissue, e.g., nuclei and lignified secondary cell walls that surround mature xylem cells in vascular bundles, while fast green is an acidic dye that will stain green the basic components of tissue, such as cytoplasm and cellulosic primary (growing) cell walls. This combination of dyes allowed us to highlight lignified tissue in xylem vessel walls (red) and cellulosic phloem cell walls (green), respectively (Ma et al., 1993). We photographed all root sections present in each slide using a Leica DM750 binocular microscope (Leica Microsystems, Wetzlar, Germany) at both 4× and 10× magnifications (Fig. 1).

We used ImageJ to identify, measure, and count individual xylem vessels (e.g., Fig. 1) and the root diameter of each root cross section. We acknowledge that, barring actual observations of water flow through vessels (e.g., through staining), it is difficult to differentiate xylem vessels that play a meaningful role in transport from those that do not. Here, we focused on larger metaxylem vessels (Kim et al., 2014), while quantifying the effect on our estimates of root transport capacity of excluding progressively smaller vessels. To do so, we located the stele in each root cross section and measured the area of the smallest identifiable red-stained xylem vessel. Using this vessel as a threshold, we ran an analysis in ImageJ to automatically identify, extract, and measure the area A of all xylem vessels larger than this reference vessel. We converted vessel area to diameter D by assuming that vessels were circular. We estimated theoretical root conductivity K_r for a given set of m vessels by using the Hagen–Poiseuille equation: $K_r = (\pi\rho/128\eta A_r)\sum_{i=1}^{m} D_i^4$, where ρ is the density of water and η is the dynamic viscosity of water (Tyree and Ewers, 1991), and A_r is root area. We included the A_r term in the equation to normalize conductivity by root area (Wang et al., 2015). We used values of ρ and η corresponding to a standard water temperature of 25°C. We plotted the cumulative value of K_r against vessel rank (from 1 to n, where n is the total number of vessels per root), with increasing rank denoting progressively smaller vessels. This method allowed us to estimate the marginal increase in root transport capacity with the addition of smaller and smaller vessels and thus estimate the error introduced by missing progressively smaller vessels (Appendix S2).

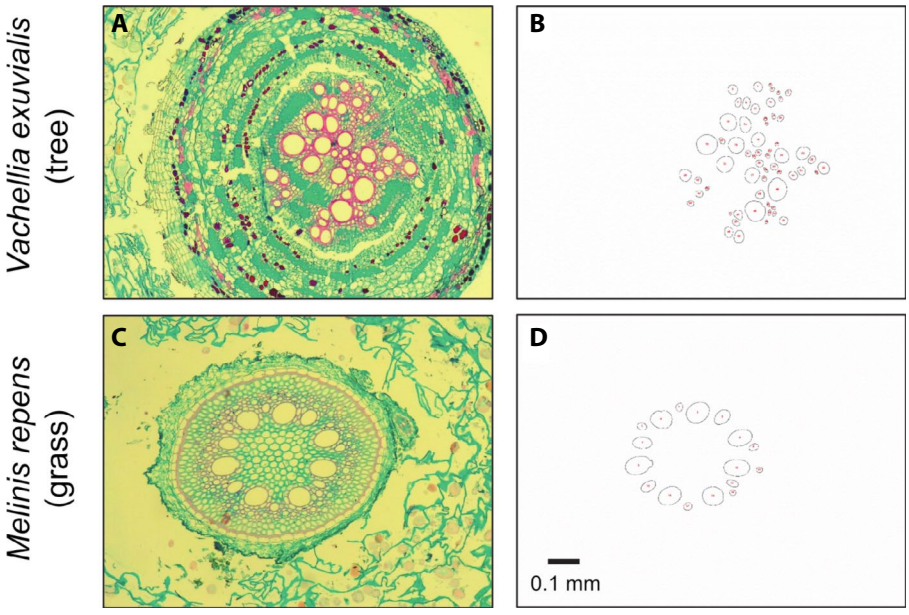

FIGURE 1. Examples of stained root cross sections (A and C) and their corresponding xylem vessels (B and D, extracted in ImageJ) for one tree (A and B: *Vachellia exuvialis*) and one grass (C and D: *Melinis repens*) species from a South African lowveld savanna ecosystem grown under greenhouse conditions.

Phylogenetic data—We obtained phylogenetic data from two sources. First, we generated a phylogenetic tree that included all of our species (trees and grasses) using scenario 1 in the V.Phylomaker R package (Jin and Qian, 2019; Qian et al., 2019). V.Phylomaker uses species lists to generate trees from published mega-trees and includes a method for attaching genera and species (for species not represented in the megatree) to close relatives in a phylogeny (Jin and Qian, 2019). Second, we trimmed a published phylogeny (Yessoufou et al., 2013) of 448 species of trees and shrubs assembled for Kruger National Park (the Kruger phylogenetic tree hereafter) to include the subset of tree species used in our study.

Statistical analyses—For each root section, we calculated six trait values that captured variation in vascular architecture. The traits were median (D_{med}) and maximum (D_{max}) vessel diameter (in mm); vessel number per unit root cross-sectional area (N, in number mm^{-2}), lumen fraction (F_l, in mm^2 mm^{-2}), vessel size to number ratio (S, in mm^4), and theoretical axial conductivity per root cross-sectional area (K_r, in kg m^{-1} MPa^{-1} s^{-1}). We used the median rather than mean vessel diameter for each root because the median is less sensitive than the mean to any missing small vessels.

Variables N, F_l, and S follow Zanne et al. (2010), except that we calculated them on the basis of individual vessel areas A_i rather than published values of mean vessel area $\overline{A}$, and we refer to F as F_l. For a root with n vessels and root cross-sectional area A_r, $N = n/A_r$, $F_l = \left(\sum_{i=1}^{n} A_i\right)/A_r$, and $S = \overline{A}/N$ (Zanne et al., 2010), where $\overline{A} = \left(\sum_{i=1}^{n} A_i\right)/n$. We calculated K_r from vessel diameters as outlined above.

We tested for the presence of a phylogenetic signal (i.e., a correlation between trait values and phylogenetic relatedness) in each of the variables (after calculating species means) using Pagel's lambda (Pagel, 1999) implemented with the phylosig function in the R phytools package. We first log-transformed values of N, F_l, S, and K_r to meet distributional assumptions. We chose the lambda statistic because it has been shown through simulation to be highly effective in discriminating random versus nonrandom trait evolution models (Münkemüller et al., 2012). We estimated phylogenetic signals for the whole phylogeny (trees plus grasses) and for trees and grasses separately. We then repeated the estimation and significance testing for the Kruger phylogeny of tree species.

To test for univariate differences in our vascular traits between trees and grasses, we used linear mixed models implemented with the lme function in the nlme package (Pinheiro and Bates, 2000), using individual roots as units of observation, treating species and individual plants within species as nested random effects and functional type as a fixed effect. The mixed models explicitly account for non-independence between observations by modeling correlations among roots within individuals and among individuals within species. In all the analyses, we combined the two subspecies of the grass *Aristida congesta* into a single species. As in the test of phylogenetic signal, we used untransformed values D_{med} and D_{max} and log-transformed values for N, F_l, S, and K_r. Acknowledging that phylogenetic correlation within functional groups for some of the variables introduces an additional level of non-independence (among closely related species), we used a conservative threshold for statistical significance ($\alpha = 0.01$). To examine vascular trait variation in a multivariate context, we conducted a principal component analysis (PCA) on the correlation matrix of the six variables (transformed where appropriate) using the prcomp function in R (R Core Team, 2020).

Given that we chose to compare trait values between the two functional groups in plants of similar size rather than age, we recognize that any trait differences had the potential to be partly confounded by plant age because our tree seedlings were older (on average) than our grasses at the time of harvest. To test whether trait values were related to plant age at harvest within the age range available in our experiment, we used linear regressions to calculate the slope of the relationship between the first principal component of the PCA and two age variables within each species: the number of days from seed sowing to harvest and the number of days from transplant to harvest. We then tested whether the mean value of the two slopes differed significantly from zero separately in each of our two functional groups.

RESULTS

Our final analysis included 539 individual root cross sections (Fig. 1) distributed across 181 of the original 197 plants (median number of cross sections per plant = 3, range = 1–4). Of the initial group, 14 individual plants died before harvest, and two sample vials were labeled incorrectly, but all of the initial species/subspecies were represented in the final collection for analysis (Appendix S1). The mean and standard deviations for estimated leaf area at harvest were 3428 ± 2735 cm^2 for grasses and 3670 ± 1991 cm^2 for trees, indicating comparable plant sizes for the two functional groups.

We found that cumulative maximum theoretical root conductivity K_r strongly asymptoted as progressively smaller vessels were considered (Appendix S2), and that the addition of the lowest ranked vessel resulted in a mean increase in maximum theoretical conductivity of 0.77% and 0.28% in individual grass and tree roots. These findings suggest that excluding some of the smallest vessels had a relatively small effect on our estimates of conductivity.

The analysis of trait phylogenetic signals suggested a significant association between trait values and phylogenetic relatedness in the V.Phylomaker tree as a whole for all six traits examined (Fig. 2; Appendix S3). When we analyzed the tree and grass clades separately, the phylogenetic signal diminished or disappeared entirely, particularly within the grass clade, suggesting that much of the association between traits and phylogeny was driven by tree–grass differences (Fig. 2; Appendix S3). Only D_{med} yielded a significant phylogenetic signal within the grass clade, while four of the six traits did so in the tree clade (Appendix S3). The results for trees were highly consistent between the V.Phylomaker and Kruger phylogenies, which produced comparable values of Pagel's lambda and similar P-values (Appendix S3).

Grasses had higher median (D_{med}: $F_{1, 38} = 40.4$, $P < 0.0001$; Fig. 3A) and maximum (D_{max}: $F_{1, 38} = 15.5$, $P < 0.001$; Fig. 3B) vessel diameters than trees, a higher lumen fraction (log F: $F_{1, 38} = 25.0$, $P < 0.0001$; Fig. 3D), higher vessel size to number ratio (log S: $F_{1, 38} = 37.5$, $P < 0.0001$; Fig. 3E) and higher estimated axial conductivity per root area (log K_r: $F_{1, 38} = 34.0$, $P < 0.0001$; Fig. 3F). Trees, in contrast, had a higher number of vessels per unit root cross section than grasses (log N: $F_{1, 38} = 10.7$, $P < 0.005$; Fig. 3C). For all variables, the standard deviations for the species and individual plant random effects were of the same order of magnitude as the residual standard deviation, showing that root trait values are correlated within individual plants and that individual trait values are correlated within species. Species-level random

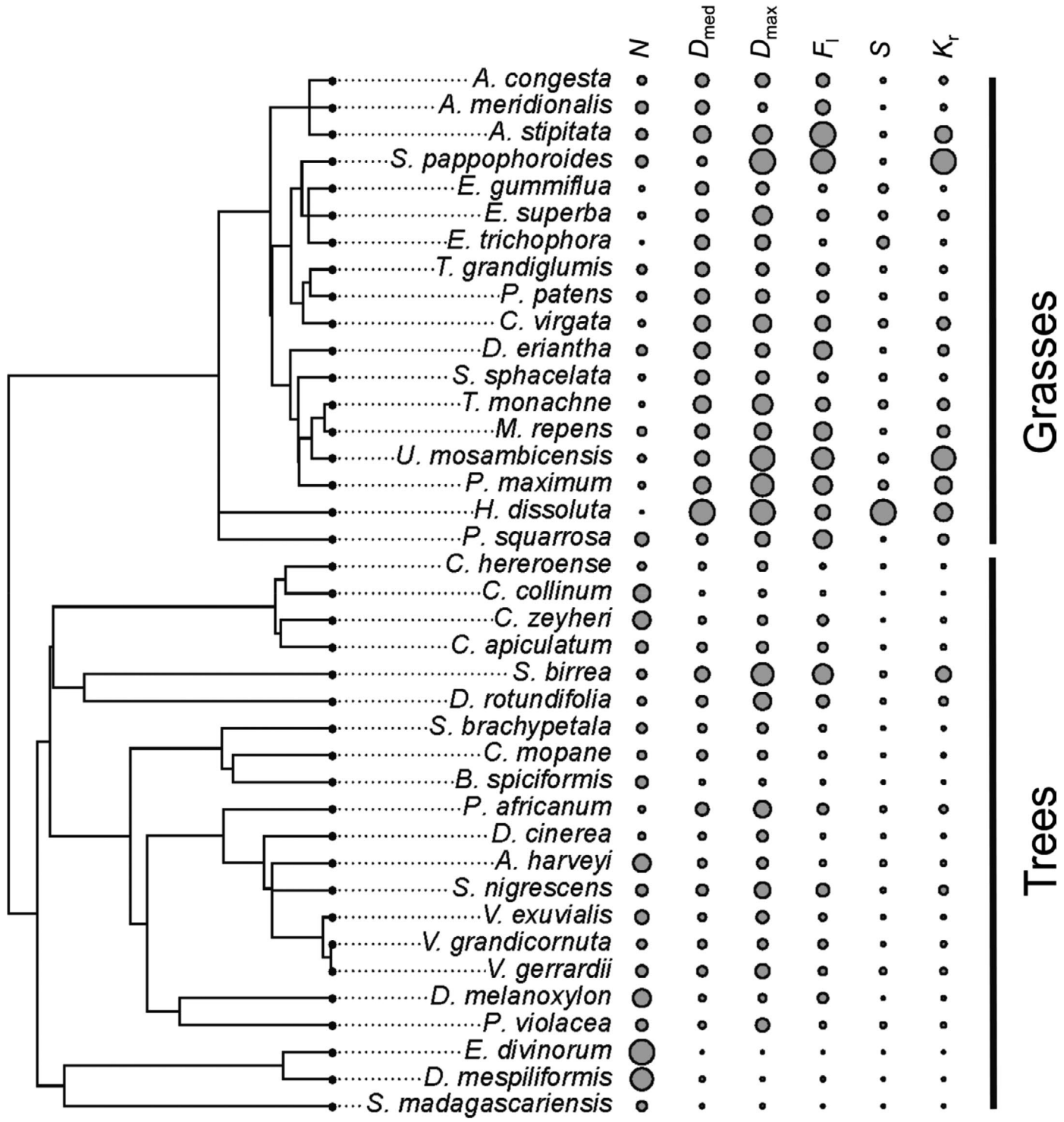

FIGURE 2. Root vascular trait values mapped across a phylogenetic tree of 21 tree (lower, primary clade) and 18 grass (upper, primary clade) species. Traits are (from left to right) vessel number per unit root cross-sectional area (*N*), median vessel diameter (D_{med}), maximum vessel diameter (D_{max}), lumen fraction (F_l), vessel size to number ratio (*S*), theoretical axial conductivity per root cross-sectional area (K_r). A full list of species is provided in Appendix S1 in Supporting Information. Circle sizes represent trait values scaled to vary between 0 and the maximum trait value within each variable.

effect standard deviations were consistently larger than individual-level standard deviations, suggesting that trait values within individual plants are less variable than trait values across individuals within species. Overall, these various differences were captured by the PCA, which segregated the two groups along the first principal component axis (Fig. 4), which accounted for 73% of the overall variance in the original variables. The first principal component separated individuals with large vessels, lumen fraction (F_l) and conductivity (K_r) from those

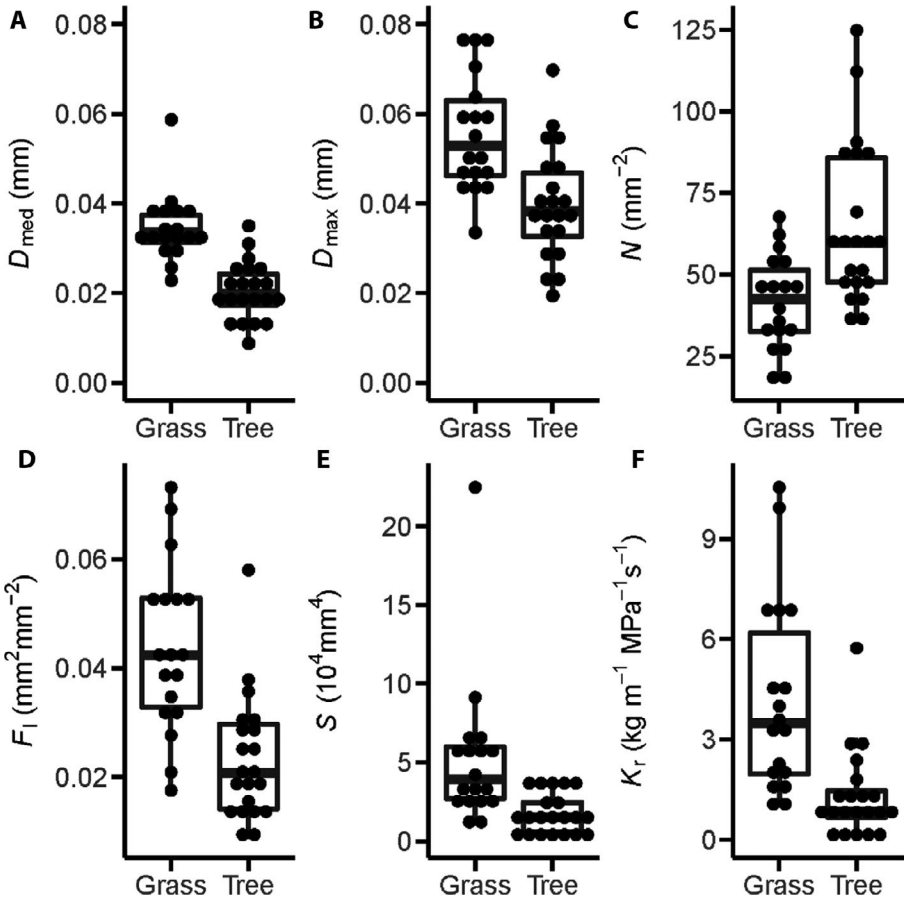

FIGURE 3. Tree–grass differences in six root vascular trait values in southern African savanna species grown under greenhouse conditions: (A) median vessel diameter (D_{med}), (B) maximum vessel diameter (D_{max}), (C) vessel number per unit root cross-sectional area (N), (D) lumen fraction (F_l), (E) vessel size to number ratio (S), and (F) theoretical axial conductivity per root cross-sectional area (K_r). Individual points represent species means.

with high vessel number per unit root cross-sectional area (N), with relatively uniform loadings across variables. The second component was more strongly driven by secondary variation in N, with positive scores on this axis indicating a smaller number of vessels per unit area.

Within species, age at harvest varied between 1 and 73 days. To include only species with a reasonable amount of age variation in our analysis of age effects, we subset the data to include those cases where the time from planting to harvest varied by more than 10 days across individuals within species (N = 22 species: 10 trees and 12 grasses). We found no evidence for a relationship between trait values (as captured by PCA axis 1) and plant age, either for trees or for grasses, whether we used the age since planting or transplanting ($P > 0.1$ in all cases); the slopes of the regressions of PC1 vs. age were distributed relatively symmetrically around 0 (Appendix S4).

Data corresponding to all root cross sections used in the analysis are provided in Appendix S5.

DISCUSSION

We found strong support for the hypothesis that savanna grass species have larger fine-root xylem vessels and conductivities than in the co-occurring trees they compete with for soil moisture. Trees have greater vessel densities than grasses do, but the aggregate theoretical transport capacity of these vessels does not offset the much stronger effect of vessel diameter in grasses. Overall, these results are consistent with the assumption that savanna grass roots have a higher capacity to transport available water than tree roots (Xu et al., 2015). This pattern was remarkably consistent across our sample of tree and grass species. If we rank all 39 species in the study by median vessel radius, then only one tree (*Sclerocarya birrea*) ranked in the top 10 species and only four (*S. birrea*, *Senegalia nigrescens*, *Dombeya rotundifolia* and *Peltophorum africanum*) in the top 20. In terms of axial conductivity (at least the fraction explained by vessel size and number), the median grass species has an estimated conductivity four times higher than the median tree species (Fig. 3F), although there is wide variation within both functional groups. Tree species, in particular, exhibited a long-tailed distribution in terms of this trait (Fig. 3F).

We found little evidence of a phylogenetic signal in root vascular traits in grasses (Fig. 2), which could be an indication that either the grass hydrological niche (e.g., rapid uptake of topsoil water) or evolutionary constraints unrelated to selective pressure limit the possible range of values for traits such as vessel size, which exhibited little interspecific variation within the grass functional group compared to trees (Fig. 2). In contrast, traits such as lumen fraction F_l and root conductivity K_r exhibited as much or more interspecific variation in grasses than in trees (Figs. 2, 3D, F), suggesting less of a constraint for these metrics. This variation, however, was not linked to phylogenetic relationships across grass clades.

Unlike the case for grasses, we found clear evidence for a phylogenetic signal in most of our vascular traits within tree species. We note, for example, that broad-leaved species in the family Combretaceae tended to exhibit small vessel diameters, while fine-leaved species in the Fabaceae (e.g., *Senegalia nigrescens* and *Peltophorum africanum*) tended to have somewhat larger vessels. The clade comprising *Euclea divinorum*, *Diospyros mespiliformis*, and *Strychnos madagascariensis* had the smallest vessel diameters. These species tend to be associated with clay-rich termite mounds and, therefore, likely experience highly negative soil matric potentials, conditions that could enhance the likelihood of cavitation and explain the investment in many small vessels (Fig. 2).

An important caveat in terms of the relationship between vessel architecture and whole-plant water use is that our current analysis is unable to quantify other important variables controlling axial conductivity, such as vessel length and pit membrane anatomy (Sperry et al., 2003; Jansen et al., 2009). Zanne et al. (2010) demonstrated that vessel size and number can provide reliable estimates

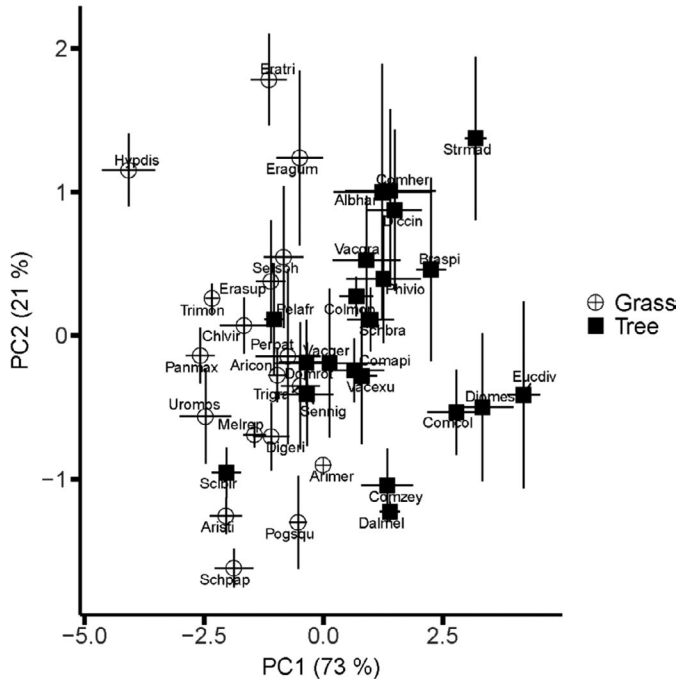

FIGURE 4. PCA scores for southern African savanna tree and grass species (mean ± SE) along the first two principal components, based on six original root vascular traits. The proportion of the overall variance explained by each axis is shown in parentheses.

of whole-stem conductivity in angiosperms. In particular, they showed that while unobserved variables such as end-wall resistivity influence conductivity, far more interspecific variation is driven by vessel cross-sectional anatomy or variables derived from them, such as F_l and S (Zanne et al., 2010). We note that the Zanne et al. (2010) study focused exclusively on stems rather than roots, and it is not clear to what extent the dominant role of vessel size and number on conductivity that they claim for stems (K_s) will apply to roots (K_r).

More generally, it is important to put these results into perspective. Ultimately, whole-root conductance depends not only on axial but on radial conductance (which we did not estimate) values of individual roots and also on traits such as specific root length and root mass ratios. For example, uptake is more dependent on root length than diameter (Craine, 2009, p. 98), so allocation of root mass to long thin roots will result in faster uptake of water within a given soil volume than allocation to short thick roots. We are currently collecting morphological root trait data for this same suite of species and quantifying whole-root conductance. This work will allow us to integrate our vessel anatomy data into a broader framework to test the power of vessel size and number data to explain whole-root conductance and plant performance.

In addition, our current work focuses on potted seedlings grown under greenhouse conditions. Further research is needed to better understand how traits measured under controlled conditions relate to traits measured under field conditions. In particular, root vessel architecture (and by implication, conductance) has been shown to vary as a function of depth in temperate grasslands (Nippert et al., 2012). Assuming the same is true in tropical savannas, a holistic understanding of tree–grass differences in water transport would require an analysis of root vascular anatomy as a function of depth. Furthermore, our results suggest that there can be a fair amount of intraspecific variation in trait values (Fig. 4) and that the amount of this variation may be greater for some species than others. We note that most of the tree species used in this analysis occur naturally in our reference study system (WRF), but seed material was collected from trees that may have experienced very different environmental conditions than those that prevail at WRF. The extent to which this geographic (and perhaps genetic) variation contributes to variation in trait values remains unknown.

Overall, our study suggests that there are potentially important functional differences in root hydraulic architecture between savanna trees and grasses. Niche-based models of tree–grass coexistence assume that functional trait trade-offs related to water use can explain this coexistence. The two-layer model assumes that grasses are superior competitors than trees for topsoil moisture, while trees have greater access to moisture in deeper layers (Walker and Noy-Meir, 1982; Eagleson and Segarra, 1985). Alternatively, the greater ability of grasses to exploit soil moisture under wet conditions might be partially offset by a growth advantage of trees under dry conditions (Xu et al., 2015). In both of these cases, grasses are assumed to have a greater ability to transport water relative to trees. Our results are consistent with this hypothesis. Ultimately, in conjunction with other key root, stem, and leaf traits, we can build whole-plant models of water use across a range of environmental conditions. Such information will allow us to identify some of the functional traits that drive differential responses of trees and grasses to changing atmospheric and soil moisture conditions, as well as move toward a clearer understanding of the ecohydrological basis of tree–grass coexistence in savannas.

CONCLUSIONS

Root vessel architecture represents just one component of the hydraulic pipeline that transports water from soils to the atmosphere. The contribution of root axial transport capacity relative to other conductivities in the transpiration pathway (e.g., root radial conductivity, stem and leaf conductivity, leaf boundary layer resistance) in savanna trees and grasses across a range of water potentials remains unclear. We have shown for the first time, however, clear differences between the two functional groups in this component of the water pipeline, with potentially important implications for our ability to predict tree–grass responses to variation in water availability.

ACKNOWLEDGMENTS

The authors thank Michael Boyd and Kevin Tarner for greenhouse support. We also thank Cameron Watt and Wits Rural Facility (University of the Witwatersrand, Johannesburg, South Africa) for facilitating access to the WRF field site. This work was funded by a CURO (Center for Undergraduate Research Opportunities) fellowship to Isabel Wargowsky and by NSF grant DEB1928860 to Ricardo Holdo. Michael Belovitch, Phoebe Judge, Cece Working, Niki Gajjar, Noemi Mazia, and two anonymous reviewers provided helpful comments on the manuscript.

DATA AVAILABILITY

Data used in the analyses for this study are provided in Appendix S5.

SUPPORTING INFORMATION

Additional Supporting Information may be found online in the supporting information tab for this article.

APPENDIX S1. List of species used in the analysis.

APPENDIX S2. Cumulative theoretical root maximum axial conductivity as a function of vessel rank.

APPENDIX S3. Tests of phylogenetic signal in six root vascular functional traits in trees and grasses combined, trees only, and grasses only.

APPENDIX S4. Distribution of within-species slopes of linear regressions of trait values (PC1) vs. plant age in trees and grasses.

APPENDIX S5. Root vascular data used in the analysis.

LITERATURE CITED

Bakker, L. M., L. Mommer, and J. van Ruijven. 2019. Using root traits to understand temporal changes in biodiversity effects in grassland mixtures. *Oikos* 128: 208–220.

Boaler, S. B., and K. C. Sciwale. 1966. Ecology of a Miombo site, Lupa North Forest Reserve, Tanzania. III. Effects on vegetation of local cultivation practices. *Journal of Ecology* 54: 577–587.

Bond, W. J. 2008. What limits trees in C_4 grasslands and savannas? *Annual Review of Ecology, Evolution and Systematics* 39: 641–659.

Craine, J. M. 2009. Resource strategies of wild plants. Princeton University Press, Princeton, NJ, USA.

Eagleson, P. S., and R. I. Segarra. 1985. Water-limited equilibrium of savanna vegetation systems. *Water Resources Research* 21: 1483–1493.

Fort, F., F. Volaire, L. Guilioni, K. Barkaoui, M.-L. Navas, and C. Roumet. 2017. Root traits are related to plant water-use among rangeland Mediterranean species. *Functional Ecology* 31: 1700–1709.

Higgins, S. I., W. J. Bond, and W. S. W. Trollope. 2000. Fire, resprouting and variability: a recipe for grass–tree coexistence in savanna. *Journal of Ecology* 88: 213–229.

Jansen, S., B. Choat, and A. Pletsers. 2009. Morphological variation of intervessel pit membranes and implications to xylem function in angiosperms. *American Journal of Botany* 96: 409–419.

Jin, Y., and H. Qian. 2019. V.PhyloMaker: an R package that can generate very large phylogenies for vascular plants. *Ecography* 42: 1353–1359.

Kim, H. K., J. Park, and I. Hwang. 2014. Investigating water transport through the xylem network in vascular plants. *Journal of Experimental Botany* 65: 1895–1904.

Lambers, H., F. S. Chapin, and T. L. Pons. 1998. Plant physiological ecology. Springer, NY, NY, USA.

Ma, Y., V. K. Sawhney, and T. A. Steeves. 1993. Staining of paraffin-embedded plant material in safranin and fast green without prior removal of the paraffin. *Canadian Journal of Botany* 71: 996–999.

Ma, Z., D. Guo, X. Xu, M. Lu, R. D. Bardgett, D. M. Eissenstat, M. L. McCormack, and L. O. Hedin. 2018. Evolutionary history resolves global organization of root functional traits. *Nature* 555: 94–97.

Münkemüller, T., S. Lavergne, B. Bzeznik, S. Dray, T. Jombart, K. Schiffers, and W. Thuiller. 2012. How to measure and test phylogenetic signal. *Methods in Ecology and Evolution* 3: 743–756.

Nippert, J. B., R. A. Wieme, T. W. Ocheltree, and J. M. Craine. 2012. Root characteristics of C_4 grasses limit reliance on deep soil water in tallgrass prairie. *Plant and Soil* 355: 385–394.

Pagel, M. 1999. Inferring the historical patterns of biological evolution. *Nature* 401: 877–884.

Pinheiro, J. C., and M. Bates. 2000. Mixed-effects models in S and S-PLUS. Statistics and Computing Series. Springer-Verlag, New York, NY, USA.

Qian, H., T. Deng, Y. Jin, L. Mao, D. Zhao, and R. E. Ricklefs. 2019. Phylogenetic dispersion and diversity in regional assemblages of seed plants in China. *Proceedings of the National Academy of Sciences* 116: 23192–23201.

R Core Team. 2020. R: A language and environment for statistical computing. R Foundation for Statistical Computing, WEIN, AUT. Website: https://www.R-project.org/.

Ratajczak, Z., P. D'Odorico, and K. Yu. 2017. The enemy of my enemy hypothesis: why coexisting with grasses may be an adaptive strategy for savanna trees. *Ecosystems* 20: 1278–1295.

Robert, E. M. R., M. Mencuccini, and J. Martinez Vilalta. 2017. The anatomy and functioning of the xylem in oaks. *In* E. Gil-Pelegrín, J. Peguero-Pina, and D. Sancho-Knapik [eds.], Oaks physiological ecology. Exploring the functional diversity of genus *Quercus* L. Tree physiology book series, vol 7, 261–302. Springer, Cham, Switzerland.

Rodríguez-Iturbe, I., P. D'Odorico, A. Porporato, and L. Ridolfi. 1999. Tree-grass coexistence in savannas: the role of spatial dynamics and climate fluctuations. *Geophysical Research Letters* 26: 247–250.

Sankaran, M., N. P. Hanan, R. J. Scholes, J. Ratnam, D. J. Augustine, B. S. Cade, J. Gignoux, et al. 2005. Determinants of woody cover in African savannas. *Nature* 438: 846–849.

Sankaran, M., J. Ratnam, and N. P. Hanan. 2004. Tree–grass coexistence in savannas revisited – insights from an examination of assumptions and mechanisms invoked in existing models. *Ecology Letters* 7: 480–490.

Schneider, C. A., W. S. Rasband, and K. W. Eliceiri. 2012. NIH Image to ImageJ: 25 years of image analysis. *Nature Methods* 9: 671–675.

Scholes, R. J., and B. H. Walker. 1993. An African savanna: synthesis of the Nylsvlei study. Cambridge University Press, Cambridge, UK.

Sperry, J. S. 2003. Evolution of water transport and xylem structure. *International Journal of Plant Sciences* 164: S115–S127.

Sperry, J. S., Y. Wang, B. T. Wolfe, D. S. Mackay, W. R. L. Anderegg, N. G. McDowell, and W. T. Pockman. 2016. Pragmatic hydraulic theory predicts stomatal responses to climatic water deficits. *New Phytologist* 212: 577–589.

Staver, A. C., S. Archibald, and S. A. Levin. 2011a. The global extent and determinants of savanna and forest as alternative biome states. *Science* 334: 230–232.

Staver, A. C., S. Archibald, and S. Levin. 2011b. Tree cover in sub-Saharan Africa: Rainfall and fire constrain forest and savanna as alternative stable states. *Ecology* 92: 1063–1072.

Tyree, M. T., and F. W. Ewers. 1991. The hydraulic architecture of trees and other woody plants. *New Phytologist* 119: 345–360.

van Wijk, M. T., and I. Rodriguez-Iturbe. 2002. Tree–grass competition in space and time: insights from a simple cellular automata model based on ecohydrological dynamics. *Water Resources Research* 38: 18–11-18-15.

Venturas, M. D., J. S. Sperry, D. M. Love, E. H. Frehner, M. G. Allred, Y. Wang, and W. R. L. Anderegg. 2018. A stomatal control model based on optimization of carbon gain versus hydraulic risk predicts aspen sapling responses to drought. *New Phytologist* 220: 836–850.

Walker, B. H., and I. Noy-Meir. 1982. Aspects of the stability and resilience of savanna ecosystems. *In* B. J. Huntley and B. H. Walker [eds.], Ecology of tropical savannas, 556–590. Springer-Verlag, Berlin, Germany.

Walter, H. 1971. Ecology of tropical and subtropical vegetation. Oliver and Boyd, Edinburgh, UK.

Wang, Y., X. Dong, H. Wang, Z. Wang, and J. Gu. 2015. Root tip morphology, anatomy, chemistry and potential hydraulic conductivity vary with soil depth in three temperate hardwood species. *Tree Physiology* 36: 99–108.

Xu, X., D. Medvigy, and I. Rodriguez-Iturbe. 2015. Relation between rainfall intensity and savanna tree abundance explained by water use strategies. *Proceedings of the National Academy of Sciences, USA* 112: 12992–12996.

Yessoufou, K., T. J. Davies, O. Maurin, M. Kuzmina, H. Schaefer, M. van der Bank, and V. Savolainen. 2013. Large herbivores favour species diversity but have mixed impacts on phylogenetic community structure in an African savanna ecosystem. *Journal of Ecology* 101: 614–625.

Yu, K., and P. D'Odorico. 2015. Hydraulic lift as a determinant of tree–grass coexistence on savannas. *New Phytologist* 207: 1038–1051.

Zanne, A. E., M. Westoby, D. S. Falster, D. D. Ackerly, S. R. Loarie, S. E. J. Arnold, and D. A. Coomes. 2010. Angiosperm wood structure: global patterns in vessel anatomy and their relation to wood density and potential conductivity. *American Journal of Botany* 97: 207–215.